

# CHARACTERIZATION AND CROSS-SECTIONAL MODELING OF THE NEWLY IDENTIFIED RAWUP FAULT BASED ON RELOCATED HYPOCENTERS AND FOCAL MECHANISM IN SOUTH SULAWESI

# Kevin Hanyu Clinton Wulur \*1,2, Joshua Purba 2, Ramadhan Priadi 2

<sup>1</sup> Program Studi Fisika, Universitas Negeri Makassar, Makassar, 9022, Indonesia,
 <sup>2</sup> Gowa Geophysical Station, Agency for Meteorology Climatology and Geophysics (BMKG), Gowa, Indonesia
 \*kevin.wulur@bmkg.go.id

Received 2025-06-24, Revised 2025-09-24, Accepted 2025-10-16, Available Online 2025-10-16, Published Regularly October 2025

### **ABSTRACT**

This study presents an integrated seismotectonic analysis combining earthquake hypocenter relocation and P-wave polarity-based focal mechanism modeling to investigate the microseismic cluster in the Maros-Pangkep region, South Sulawesi. Using seismic data recorded by the BMKG network between 2019 and 2024, a total of 191 events were successfully relocated through the double-difference (HypoDD) algorithm, achieving a significant reduction in RMS residuals. The relocated hypocenters delineate a coherent northwest-southeast-trending fault plane with a strike of approximately 260° and a dip of 7–9°, consistent with a dextral strike-slip mechanism exhibiting minor oblique components. Integration with polarity-derived focal mechanisms confirms a consistent stress orientation compatible with regional compression along the Walanae Fault System. This alignment suggests the presence of a previously unmapped active structure, herein referred to as the Rawup Fault, accommodating local stress redistribution between carbonate and volcanic-clastic units. The findings advance the understanding of active deformation in low-seismicity, karst-dominated terrains and demonstrate the value of combining relocation and focal mechanism analyses for detecting hidden faults. These results provide new insights into the tectonic evolution and seismic hazard potential of the Maros-Pangkep.

Keywords: Hypocenter relocation; Double-difference; Focal Mechanism; Rawup fault; Maros-Pangkep.

# INTRODUCTION

Sulawesi Island lies at the triple junction between the Eurasian, Indo-Australian, and Pacific plates (Figure 1a), resulting in a complex pattern of crustal deformation and fault segmentation across the region. The island accommodates a series of strike-slip, thrust, and normal faults that form an intricate tectonic framework, including the Palu–Koro, Matano, and Walanae fault systems [1-6]. Among these, the Walanae Fault—extending for more than 150 km—represents a major transcurrent structure dividing South Sulawesi into several crustal blocks with contrasting deformation styles [4-10].

The adjacent Maros–Pangkep region, located approximately 50 km west of the Walanae Fault, is characterized by extensive tropical karst topography developed within Eocene–Miocene limestone of the Tonasa Formation [11-12]. Despite being considered tectonically stable, this area has recently exhibited an anomalous increase in microseismic activity recorded by the BMKG Gowa Seismic Network [13], suggesting the presence of shallow crustal deformation processes not directly associated with mapped major faults.

Karst terrains are mechanically sensitive to stress perturbations due to the heterogeneous nature of carbonate–clastic lithological contacts and the presence of pre-existing discontinuities <sup>[14]</sup>. In such carbonate-dominated regions, microcrack propagation is commonly driven by localized stress concentrations that are amplified along lithological boundaries and fracture networks <sup>[15]</sup>. Numerous studies have shown that microseismic clusters in carbonate crusts can reveal the development of hidden fault segments or diffuse deformation zones that act as conduits for stress redistribution <sup>[16]</sup>. These features are particularly relevant to the Maros–Pangkep karst province, where repeated microseismic events may signal the evolution of weak zones that have not yet ruptured at the surface <sup>[13]</sup>.

To resolve the geometry of such deformation zones, earthquake hypocenter relocation is a powerful approach for improving spatial precision and delineating clustered seismicity [3, 17-20]. The double-difference (DD) algorithm, implemented in HypoDD, compares the differential travel times between pairs of nearby events to minimize velocity-model errors and refine hypocenter distributions. Integration of relocation with three-dimensional (3D) velocity models significantly enhances the ability to characterize fault geometries, rupture planes, and stress-transfer pathways in both high- and low-seismicity regions [3, 17-20]. Recent developments in 3D cross-sectional and voxel-based modeling techniques have allowed researchers to visualize fault architecture and microcracking pathways more realistically, bridging the gap between seismic observation and structural [14, 21-22].

While relocation techniques refine the spatial distribution of seismicity, focal mechanism analysis provides essential constraints on fault orientation, slip direction, and prevailing stress regime <sup>[23-24]</sup>. Determining focal mechanisms from P-wave first-motion polarity is particularly valuable for low-magnitude events, where full moment-tensor inversion is often infeasible <sup>[25-26]</sup>. Recent developments in automated polarity analysis and machine-learning approaches have further improved the accuracy of focal mechanism solutions in sparse seismic networks <sup>[27]</sup>. By integrating relocated hypocenters with polarity-based focal mechanisms, it becomes possible to construct three-dimensional models of fault planes and to infer stress orientations responsible for the observed seismic activity <sup>[28-29]</sup>.

In low-seismicity zones, such as the Maros–Pangkep region, precise relocation of microseismic events can reveal subtle stress redistribution and early-stage fault reactivation that are often missed by conventional analyses [30-31]. This is critical in Sulawesi, where tectonic stress transfer from the Walanae system may interact with secondary faults and lithological discontinuities, creating complex zones of deformation [13, 32]. Understanding these subtle deformation patterns is essential for updating regional fault maps and assessing seismic hazards in areas previously considered quiescent. The analysis of clustered microearthquakes in the Maros–Pangkep region, when coupled with P-wave polarity data, reveals consistent orientations of compressional and tensional quadrants, indicating the presence of a coherent fault plane distinct from the main Walanae trace.

The combination of hypocenter relocation and focal mechanism analysis offers an effective framework for identifying and characterizing hidden fault structures in low-seismicity regions such as Maros–Pangkep. Relocation enhances the spatial accuracy of clustered seismicity,

while P-wave polarity—based focal mechanisms constrain fault orientations and slip directions, providing a more complete understanding of the local stress field. When applied together, these techniques can distinguish diffuse microcracking from organized faulting and help to infer subsurface geometries of emerging deformation zones within carbonate-dominated crusts.

This study applies an integrated relocation—focal mechanism approach to investigate shallow crustal deformation beneath the Maros—Pangkep region, South Sulawesi. Through three-dimensional cross-sectional modeling, the research aims to delineate the geometry, kinematics, and stress regime of the observed seismic cluster and to evaluate its relationship with the Walanae system and surrounding lithological boundaries. The investigation is expected to reveal whether the cluster represents a localized stress redistribution zone or an evolving fault segment—one that may later be referred to as the Rawup Fault—thereby contributing to a refined understanding of fault segmentation and seismic hazard in the tectonically complex crust of South Sulawesi.

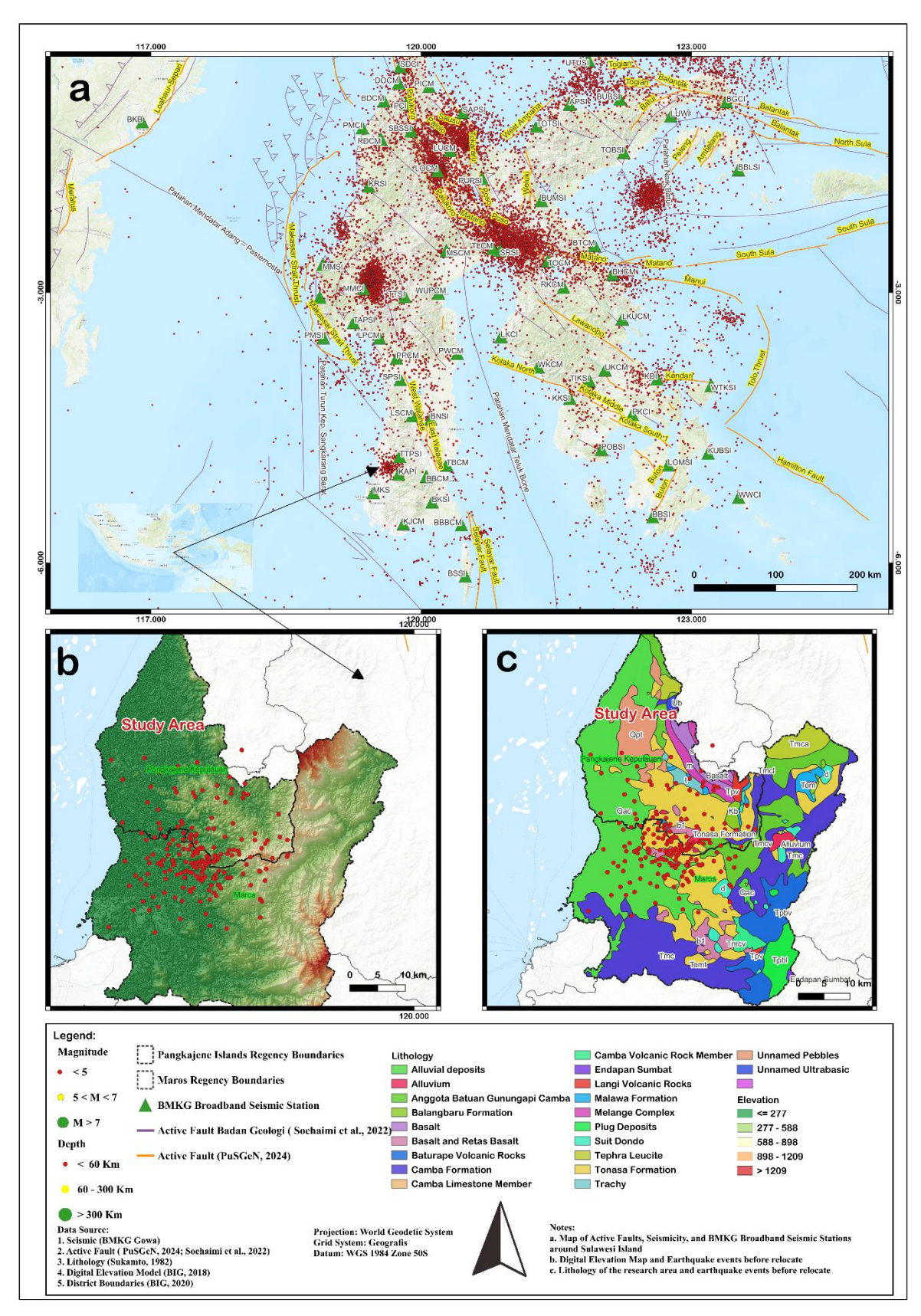


**Figure 1.** a) Map of Active Faults and BMKG Broadband Seismic Stations around Sulawesi Island, b) Digital Elevation Model and Seismicity of the Maros-Pangkep region and its surroundings, c) Lithology of the research area and earthquake events before relocation (195 events)

### **METHOD**

# Seismic Data and Study Area

This study utilized digital seismic records obtained from the broadband seismic network of the Meteorology, Climatology, and Geophysics Agency (BMKG), Gowa Geophysical Station, covering the period from 2019 to 2024 (Figure 1a). The dataset consisted of P- and S-wave arrival times automatically processed by the SeisComP4 system and manually reviewed for quality control. The study area is bounded by coordinates 4°45′–5°03′36″S and 119°27′–119°49′12″E, encompassing the Maros–Pangkep karst province of South Sulawesi.

The network configuration, which includes several broadband stations distributed across South Sulawesi (Figure 3), ensures a reasonable azimuthal coverage for local seismicity. Only events with a minimum of four high-quality phase picks and reliable signal-to-noise ratios were retained. These criteria were essential for minimizing travel-time uncertainty in the relocation stage. Initial event locations were computed using the LocSAT algorithm [33] within the SeisComP4 framework [34], employing the global IASP91 velocity model [35-36] as the initial reference for travel-time calculations. Although this model does not represent the local velocity heterogeneity of Sulawesi's crust, the IASP91 model was selected because it offers a robust, time-tested baseline for global and regional traveltime predictions and event-location procedures. Compared to more recent models such as AK135, which was developed for improved global traveltime fits and compatibility with normal-mode data [36-38] IASP91 remains advantageous in regional studies where stability, simplicity, and consistency are prioritized. Its 1-D velocity structure—derived from a comprehensive compilation of regional and teleseismic P- and S-wave travel times—provides reliable first-order corrections for crustal and upper-mantle paths, particularly in regions with limited local calibration [39-40]. Thus, IASP91 serves as a dependable reference for initial event locations prior to applying highresolution relocation techniques such as the double-difference method.

### Hypocenter Double-Difference (HypoDD) and Focal Mechanism

This study employs an integrated workflow combining hypocenter relocation using the double-difference (DD) method and focal mechanism analysis derived from P-wave first-motion polarity to characterize shallow crustal deformation in the Maros–Pangkep region. Hypocenter relocation was performed using the HypoDD algorithm  $^{[41-42]}$ , which minimizes velocity-model errors by comparing the differential travel times between pairs of nearby earthquakes recorded at common seismic stations. Two closely spaced earthquakes that share nearly identical ray paths will exhibit similar travel times; therefore, the difference in their arrival times primarily reflects the difference in their source locations. The residual travel time between two earthquakes i and j recorded at station k is expressed as:

$$d_k^{ij} = (t_k^i - t_k^j)^{obs} - (t_k^i - t_k^j)^{cal}$$
(1)

Where:

 $t_k^i$  and  $t_k^j$  denote the observed and calculated travel times of seismic waves from events i and j to station k, respectively. By differentiating the travel time with respect to the model parameters, the equation becomes:

$$\Delta d = \frac{\partial t_k^i}{\partial m} \Delta m^i - \frac{\partial t_k^j}{\partial m} \Delta m^j \tag{2}$$

and when expanded into three-dimensional space:

$$\Delta d = \frac{\partial t_k^i}{\partial x} \Delta x^i + \frac{\partial t_k^i}{\partial y} \Delta y^i + \frac{\partial t_k^i}{\partial z} \Delta z^i + \Delta t_0^i - \frac{\partial t_k^j}{\partial x} \Delta x^j - \frac{\partial t_k^j}{\partial y} \Delta y^j - \frac{\partial t_k^j}{\partial z} \Delta z^j - \Delta t_0^j$$
(3)

which in matrix form is written as:

$$W\Delta d = WG\Delta m \tag{4}$$

### Where:

 $\Delta d$  represents the vector of travel-time residuals, G is the Jacobian matrix containing the partial derivatives of hypocentral parameters,  $\Delta m$  is the vector of location adjustments, and W is a weighting matrix that controls the contribution of each observation [43-44]. The solution is obtained iteratively using singular value decomposition (SVD) to minimize the least squares of residuals until convergence [45]. The maximum distance between earthquake pairs within a cluster was set to 10 km, with a maximum of six neighbors per event. Each pair was required to have at least four linked stations, and the maximum station distance from the cluster centroid was limited to 200 km. Only events showing consistent P- and S-wave arrivals were retained to ensure stable relocation results.

The relocated hypocenters were subsequently analyzed to determine focal mechanisms using P-wave first-motion polarity recorded by the BMKG seismic network <sup>[13]</sup>. For each event, the polarity of the initial P-wave motion—whether compressional (up) or dilatational (down)—was manually verified to minimize phase misidentification. The combination of multiple polarities from spatially distributed stations enabled the determination of nodal planes representing potential fault orientations and slip directions. These focal mechanisms were then cross-correlated with the relocated hypocenter clusters to infer the prevailing stress regime and the geometry of the active deformation zone. By integrating the HypoDD relocation results with polarity-based focal mechanisms within a three-dimensional modeling framework, this study aimed to constrain the orientation, dip, and sense of movement of a previously unmapped structure that may later be referred to as the Rawup Fault. This combined approach provides a robust foundation for characterizing the geometry and kinematics of shallow crustal deformation in South Sulawesi and for assessing the seismotectonic significance of emerging fault systems in carbonate-dominated terrains.

### **Validation and Uncertainty Estimation**

The reliability of the relocation results was assessed through the analysis of the root mean square (RMS) residuals between observed and calculated travel times. The RMS value serves as a quantitative indicator of model consistency, where a lower RMS reflects improved agreement between the observed and modeled arrival times. A comparison of RMS histograms before and after relocation demonstrates that the double-difference method substantially reduces spatial uncertainty, leading to a more coherent clustering of hypocenters.

For the focal mechanism solutions, validation was performed by examining the polarity misfit rate between the observed and predicted P-wave first motions. Only mechanisms with less than 10% polarity misfit were accepted. Additionally, the preferred fault plane from the focal mechanism was cross-checked against the orientation of the relocated hypocenter alignment to ensure geometric consistency. The convergence of these independent datasets—relocation and polarity-derived mechanisms—supports the robustness of the interpreted fault geometry.

This combined validation framework, involving both RMS residual analysis and polarity consistency checks, ensures that the relocated hypocenters and focal mechanism solutions provide a reliable representation of the active fault structure within the study area.

### **RESULTS AND DISCUSSION**

## **Hypocenter Relocation and Cluster Geometry**

A total of 191 microearthquake events recorded by the BMKG network between 2019 and 2024 were successfully relocated using the double-difference (HypoDD) algorithm. This process utilized P- and S-wave phases and significantly reduced RMS residuals, with most post-relocation values ranging from -0.8 to 0.8 seconds (Figure 2), indicating a marked increase in location precision. The resulting hypocenter distribution (Figure 3) forms a well-defined cluster trending northwest–southeast with a strike of approximately  $260^{\circ}$  and a dip of  $7-9^{\circ}$ .

Such relocation-based clustering is a robust approach for revealing hidden or reactivated fault structures in low-to-moderate seismicity regions [13, 46-47]. The HypoDD method, through iterative refinement of differential travel times, effectively minimizes velocity-model bias and improves fault-plane definition even in sparse networks [48]. In similar studies, relocated microseismic events have delineated subtle strike-slip zones in carbonate and volcanic terrains, highlighting that such clusters are reliable indicators of local fault reactivation processes [13, 47].

Waveform data from nearby seismic stations (e.g., KAPI, TTPSI, and BBCM) display sharp P-wave onsets and consistent first-motion polarity across multiple events within the Maros-Pangkep cluster (Figure 3). Stations KAPI and TTPSI, located closest to the seismic source, display high amplitudes, suggesting a shallow source depth and relatively strong initial energy release. In contrast, stations BKSI (intermediate distances) recorded lower amplitudes and delayed arrivals, consistent with energy attenuation during wave propagation. Distant stations BNSI and KJCM show more subdued P-phases, implying heterogeneous crustal transmission paths. The P-arrival polarity patterns suggest a dominant strike-slip mechanism with minor reverse (oblique) components, consistent with compressional stress acting in the upper crust.

Determining focal mechanisms through P-wave first-motion polarity remains a widely adopted method for low-magnitude events where full moment-tensor inversion is infeasible <sup>[24, 49]</sup>. The integration of relocated hypocenters and polarity-based mechanisms allows precise inference of the active fault plane and slip direction, even within limited station coverage <sup>[13, 47]</sup>. The

observed dextral (right-lateral) shear motion aligns with regional stress regimes associated with the transcurrent fault systems of South Sulawesi, supporting the interpretation that this cluster corresponds to a shallow, strike-slip-dominated fault zone.

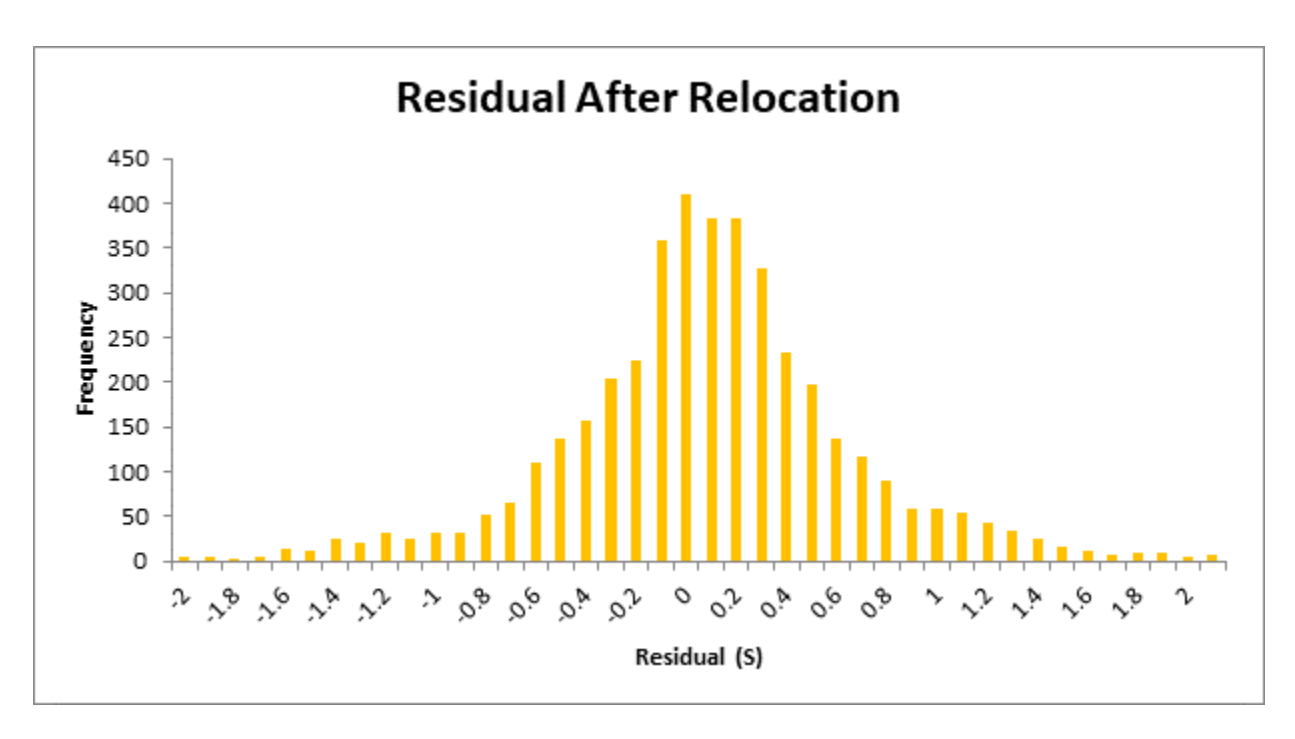
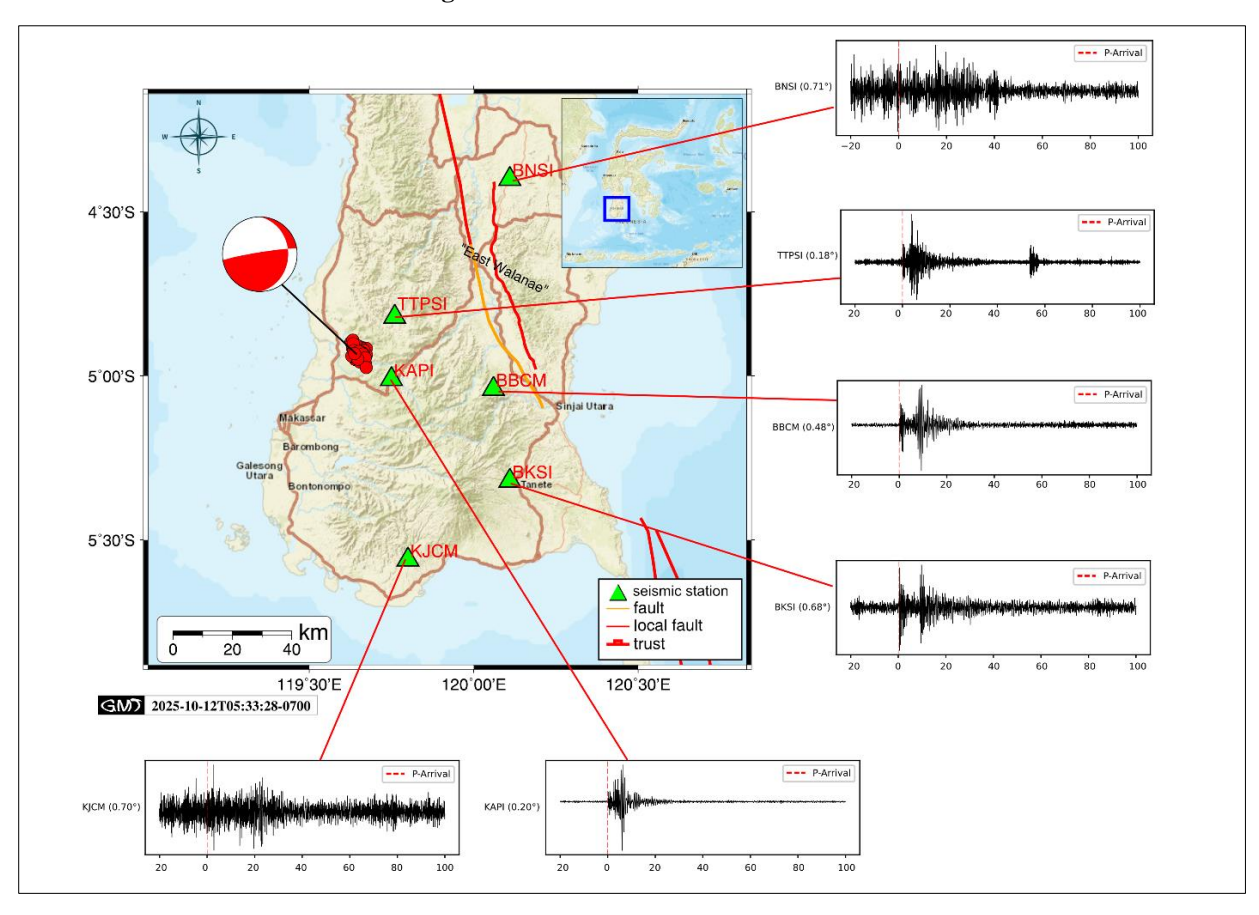


Figure 2. Residual Value after relocation.



**Figure 3.** Representative waveform and Focal Mechanism of a microearthquake event from the Maros–Pangkep cluster recorded at several BMKG stations. The sharp P-wave onset and consistent first-motion polarities support a strike-slip faulting mechanism.

### **Fault Geometry Modeling and Seismotectonic Interpretation**

Three-dimensional visualization of the relocated hypocenters projected onto a digital elevation model (DEM) shows that the seismic cluster extends linearly along a northwest—southeast trend with depths predominantly less than 10 km (Figure 4). This pattern corresponds spatially with the transitional zone between uplifted karst hills and lower structural valleys in the Maros—Pangkep area. The alignment of seismicity along this morphotectonic boundary indicates that surface morphology in the karst terrain is strongly controlled by subsurface faulting and differential uplift.

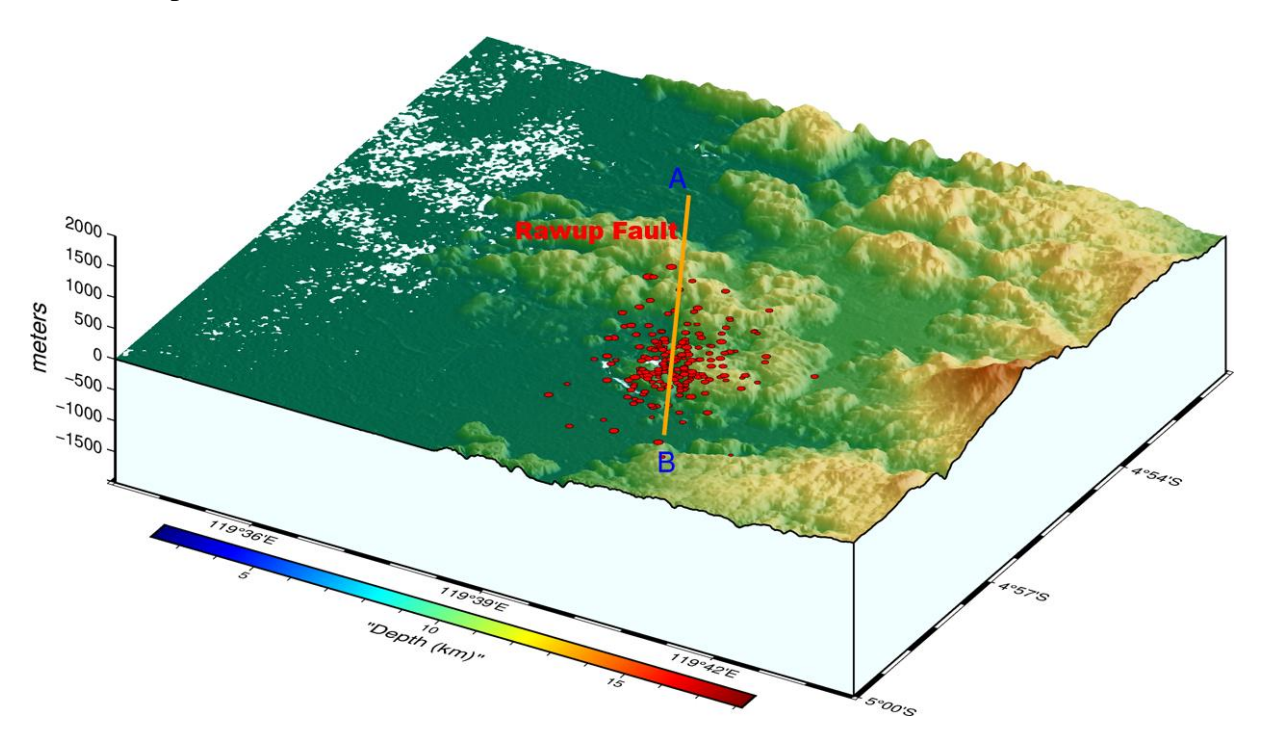


**Figure 4.** Three-dimensional DEM map of the Maros–Pangkep seismic cluster. Red dots indicate relocated hypocenters, showing a linear northwest–southeast alignment parallel to the Rawup Fault. The topography illustrates the relationship between fault geometry and karst landscape deformation. Orange line shows estimated fault location.

A 3D fault-plane model was constructed from the spatial distribution of relocated hypocenters (Figure 5). The modeled fault surface dips gently southward ( $\approx$ 7°) with a strike of about 260°, consistent with the strike-slip focal mechanism derived from P-wave polarity data (Figure 3). The hypocenters align along this surface to depths of ~10 km, representing a seismically active deformation zone in the upper to middle crust. Regionally, the Rawup Fault is interpreted as a synthetic structure related to the Walanae Fault System, which accommodates transcurrent motion between the relatively stable Makassar Block to the west and the uplifting Bone–Pangkep Block to the east [4-10, 30-31]. The shallow dip and strike-slip nature of the Rawup Fault suggest that it functions as a subsidiary shear zone, likely reactivated along pre-existing lithological boundaries between the Tonasa carbonate formation and Camba volcanic–clastic units [3-4, 50-54].

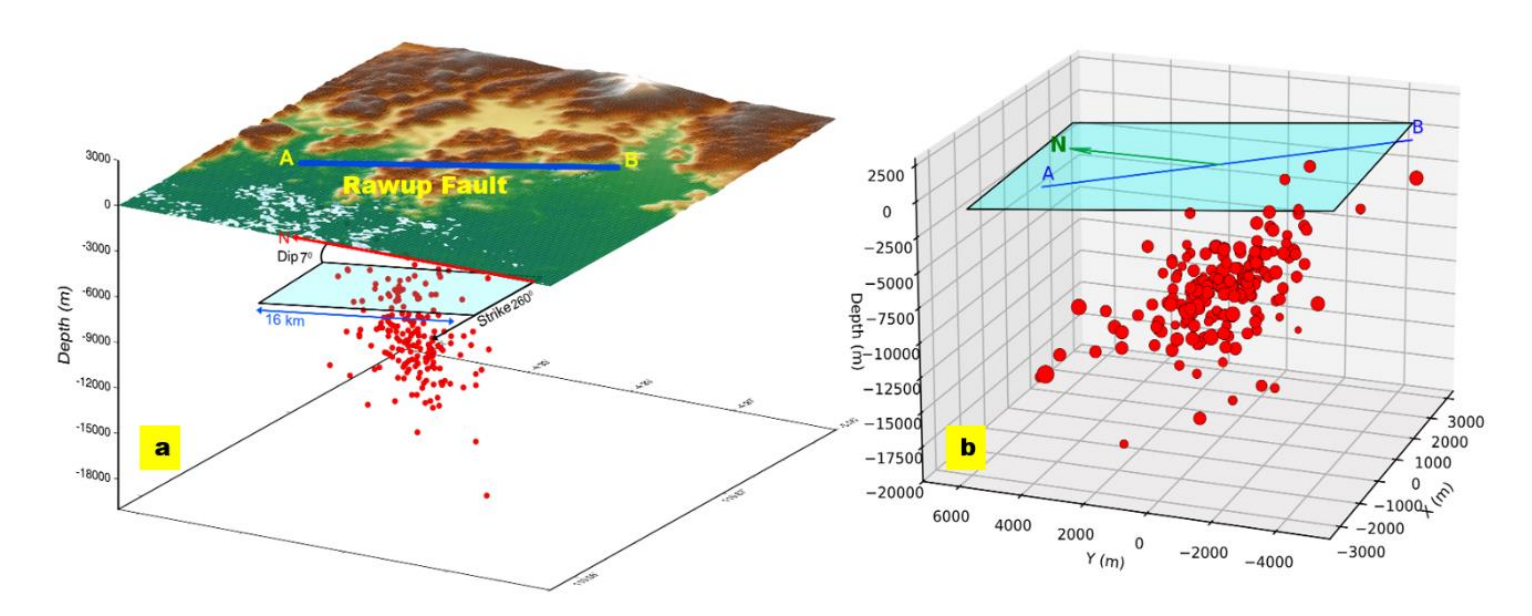


**Figure 5.** Interpreted Rawup Fault plane based on relocated hypocenters: a) 3D projection over DEM showing surface correlation, b) cross-sectional model highlighting the fault geometry with a strike of  $\sim 260^{\circ}$  and dip of  $\sim 7^{\circ}$ . Blue plane = inferred fault surface; red points = relocated hypocenters; blue line = shows estimated fault.

The concentration of relocated hypocenters at the lithological boundary between the Tonasa Formation (massive Eocene-Miocene limestone) and the Camba Formation (volcanic-clastic unit) as shown on figure 1c suggests that local mechanical contrasts strongly influence the localization of seismic deformation [3-4, 50-54]. Laboratory and field-based studies indicate that contrasts in rock competency and elasticity govern how stress is accommodated and released in the upper crust [55-58]. In carbonate-dominated terrains, deformation tends to be concentrated along discontinuities where microcracks and small-scale slip surfaces propagate preferentially [59-60]. These microcracks act as precursors to fault nucleation under low differential stress conditions, a phenomenon well-documented in karst environments [13, 61-63]. The Maros-Pangkep karst region, composed of alternating limestone from the Tonasa Formation and volcanic—clastic deposits of the Camba Formation, provides an ideal setting for localized strain accumulation and small-scale fault reactivation. The mechanical contrast between these rocks exerts strong control on stress concentration and deformation style in the upper crust. Laboratory studies indicate that limestone exhibits lower compliance and higher rigidity than sandstone, influencing effective pressure and fluid migration [64-65]. Sandstone, with greater porosity, tends to weaken when saturated, while limestone undergoes inelastic compaction under stress [66]. Consequently, the lithological interface between these contrasting units forms a mechanically weak discontinuity that promotes slip initiation and microcrack propagation, consistent with the observed seismic clustering in the Maros–Pangkep area.

The spatial distribution, focal mechanism, and structural alignment of the Maros–Pangkep seismic cluster indicate the presence of a previously unmapped fault zone, herein referred to as the Rawup Fault. This fault trends northwest–southeast (strike  $\approx 260^{\circ}$ ) and dips gently to the southwest, showing characteristics consistent with a dextral strike-slip system. The orientation of the Rawup Fault aligns subparallel to the East Walanae Fault, suggesting it functions as a subsidiary or synthetic structure accommodating transcurrent motion within the same regional stress field [30, 49]). This interpretation supports the notion that South Sulawesi's crustal

deformation is governed by oblique convergence and microplate rotation, producing complex transpressional faulting patterns <sup>[47, 49]</sup>. The relatively shallow hypocenter distribution (< 10 km) indicates that deformation occurs within the brittle upper crust, consistent with secondary fault reactivation along pre-existing structural weaknesses formed during past obduction and uplift of oceanic crustal material <sup>[13, 61-63]</sup>.

The interpreted Rawup Fault exhibits an estimated fault length of  $\pm$  11 km and a width of  $\pm$  6 km. Applying the empirical scaling relationship from Wells and Coppersmith <sup>[67]</sup>, the corresponding moment magnitude is estimated at Mw  $\approx$  6.2, suggesting that this fault has the potential to generate moderate to strong earthquakes if rupture occurs along its full extent. Similar scaling relations for strike-slip faults in Southeast Asia show comparable magnitudes for faults of similar dimensions <sup>[68, 69]</sup>. Although current seismicity in the Maros–Pangkep region is dominated by microearthquakes, the identified fault geometry and regional stress field imply that the Rawup Fault is an active structure with non-negligible seismic potential. These findings are crucial for updating regional fault maps and improving seismic hazard assessment in areas previously considered tectonically stable <sup>[70]</sup>.

The integration of relocated hypocenter data, waveform polarity analysis, and geological constraints thus provides a comprehensive model for understanding ongoing crustal deformation in the Maros–Pangkep area. The Rawup Fault likely represents a near-surface manifestation of continuing tectonic adjustment within the Walanae–Bone deformation corridor. Moreover, the strong lithological influence and shallow hypocenter depths indicate that deformation is concentrated within carbonate-rich units, consistent with studies of microseismic reactivation in carbonate terrains [13, 59-63]. Collectively, these results affirm that the Maros–Pangkep region is an active tectonic zone rather than a seismically quiescent one. Continued microseismic monitoring and high-resolution geophysical mapping are essential to fully characterize the Rawup Fault system and to mitigate potential seismic hazards in South Sulawesi.

# **CONCLUSION**

This study integrates high-resolution hypocenter relocation with P-wave polarity-based focal mechanism analysis to characterize an active shallow fault system in the Maros-Pangkep region of South Sulawesi. The combined approach successfully delineated a coherent northwest-southeast-trending seismic cluster, defining a fault plane with a strike of approximately 260° and a gentle dip of 7–9°, indicative of a dextral (right-lateral) strike-slip mechanism with minor oblique components. The spatial consistency between relocated hypocenters, focal mechanism orientations, and surface morphology provides strong evidence for the presence of a previously unrecognized fault structure, herein referred to as the Rawup Fault. This fault is interpreted as a shallow crustal deformation zone accommodating local stress redistribution derived from the Walanae Fault System and amplified by mechanical contrasts between the Tonasa carbonate and Camba volcanic-clastic formations. The identification and 3D modeling of the Rawup Fault highlight the effectiveness of integrating hypocenter relocation and focal mechanism data for detecting hidden active faults in lowseismicity, carbonate-dominated terrains. These findings contribute to refining the regional seismotectonic framework of South Sulawesi and underscore the importance of continued seismic monitoring and detailed geological mapping to improve hazard assessment and fault characterization in Eastern Indonesia. Future research should focus on integrating focal mechanism inversions with local 3D velocity models and dense seismic arrays to improve

constraint on stress-field heterogeneity and rupture dynamics along the Rawup Fault. Incorporating geodetic data, such as Lidar and GNSS, could further quantify surface deformation and slip rates, while paleoseismological and structural field investigations are recommended to validate subsurface fault geometries inferred from seismic data. Such multidisciplinary efforts will enhance understanding of active deformation processes in carbonate terrains and refine seismic hazard assessments across South Sulawesi.

# **ACKNOWLEDGMENTS**

The author gratefully acknowledges Papa Harimau Project from the Gowa Geophysical Station, Agency for Meteorology, Climatology, and Geophysics (BMKG) for their support during this research. Their assistance in providing seismic data and technical insights was instrumental in the successful completion of the hypocenter relocation analysis and seismotectonic interpretation in this study.

### **REFERENCES**

- Irsyam, M., Cummins, P. R., Asrurifak, M., Faizal, L., Natawidjaja, D. H., Widiyantoro, S., Meilano, I., Triyoso, W., Rudiyanto, A., Hidayati, S., Ridwan, M., Hanifa, N. R., & Syahbana, A. J. (2020). Development of the 2017 national seismic hazard maps of Indonesia. Earthquake Spectra, 36(1\_suppl). https://doi.org/10.1177/8755293020951206.
- Perston, Y. L., Sumantri, I., Hakim, B., Oktaviana, A. A., & Brumm, A. (2020). Excavation report for leang rakkoe: a new toalean site with engraved art in the bomboro valley, maros regency, south sulawesi. Jurnal walennae, 18(1). https://doi.org/10.24832/wln.v18i1.427.
- Purba, J., Priadi, R., Frando, M., & Pertiwi, I. (2025). The Purpri Fault: A newly identified active fault in East Kolaka, Indonesia, based on HypoDD and DInSAR. Geoloski Anali Balkanskoga Poluostrva, 00, 5–5. https://doi.org/10.2298/GABP250417005P.
- Jaya, A., & Nishikawa, O. (2013). Paleostress reconstruction from calcite twin and fault-slip data using the multiple inverse method in the East Walanae fault zone: Implications for the Neogene contraction in South Sulawesi, Indonesia. *Journal of Structural Geology*, 55. https://doi.org/10.1016/j.jsg.2013.07.006.
- Jaya, A., Nishikawa, O., & Jumadil, S. (2023). Paleoseismic Analysis of the Walanae Fault Zone in South Sulawesi, Indonesia. Indonesian Journal on Geoscience, 10(2). https://doi.org/10.17014/ijog.10.2.215-227.
- Justia, M., Hiola, M. F. H., & Febryana S, N. B. (2018). Gravity anomaly to identify Walanae fault using second vertical derivative method. Journal of Physics: Theories and Applications, 2(1). https://doi.org/10.20961/jphystheor-appl.v2i1.29008.
- Sarsito, D. A., Susilo, S., Rudyawan, A., Muhammad, N. A., Andreas, H., & Pradipta, D. (2019). Walanae fault kinematic deduced from geometric geodetic gnss GPS monitoring. E3S Web of Conferences, 94. https://doi.org/10.1051/e3sconf/20199404008.
- Safani, J., Ibrahim, K., Deni, W., Rubaiyn, A., Firdaus, F., & Harisma, H. (2023). Interpreting structural configuration of the Sengkang Basin of Indonesia using edge detection and 3-D Euler deconvolution to satellite gravity data. Turkish Journal of Earth Sciences, 32(7). https://doi.org/10.55730/1300-0985.1881.
- Suyono, S. (2010). Stratigraphy and Tectonics of the Sengkang Basin, South Sulawesi. Indonesian Journal on Geoscience. https://doi.org/10.17014/ijog.vol5no1.20101.
- PuSGeN. (2024). Peta Sumber dan Bahaya Gempa Indonesia Tahun 2024 [Map of Indonesia Earthquake Sources and Hazards in 2024- in Indonesian]. PUPR Press, 515 pp.
- Wilson, M. E. J., Bosence, D. W. J., & Limbong, A. (2000). Tertiary syntectonic carbonate platform development in Indonesia. Sedimentology, 47(2). https://doi.org/10.1046/j.1365-3091.2000.00299.x.
- Huntley, J., Aubert, M., Oktaviana, A. A., Lebe, R., Hakim, B., Burhan, B., Aksa, L. M., Geria, I. M., Ramli, M., Siagian, L., Brand, H. E. A., and Brumm, A. 2021. The effects of climate change on the Pleistocene rock art of Sulawesi. Scientific Reports, 11(1). https://doi.org/10.1038/s41598-021-87923-3.

- Wulur, K., H, C., Junaedi, S., Susanto, A., Purba, J., & Priadi, R. (2025). Hypocenter relocation to identify hidden faults and their environmental implications in the karst region of Maros-Pangkep, South Sulawesi. Journal Of Degraded and Mining Lands Management, 12(5), 8663–8676. https://doi.org/10.15243/jdmlm.2025.125.8663.
- Diehl, T., Kissling, E., Herwegh, M., & Schmid, S. M. (2021). Improving absolute hypocenter accuracy with 3d pg and sg body-wave inversion procedures and application to earthquakes in the central alps region. Journal of Geophysical Research: Solid Earth, 126(12). https://doi.org/10.1029/2021jb022155.
- Lomax, A. and Savvaidis, A. (2021). High-precision earthquake location using source-specific station terms and inter-event waveform similarity. Journal of Geophysical Research: Solid Earth, 127(1). https://doi.org/10.1029/2021jb023190.
- Trugman, D. T., Chamberlain, C. J., Savvaidis, A., & Lomax, A. (2022). Growclust3d.jl: a julia package for the relative relocation of earthquake hypocenters using 3d velocity models. Seismological Research Letters, 94(1), 443-456. https://doi.org/10.1785/0220220193.
- Waldhauser, F., & Ellsworth, W. L. (2000). A Double-difference Earthquake location algorithm: Method and application to the Northern Hayward Fault, California. Bulletin of the Seismological Society of America, 90(6): 1353–1368. https://doi.org/10.1785/0120000006.
- Waldhauser, F. (2001). Hypodd-a program to compute double-difference hypocenter locations. Open-File Report. https://doi.org/10.3133/ofr01113.
- Supendi, P., Nugraha, A. D., Widiyantoro, S., Abdullah, C. I., Puspito, N. T., Palgunadi, K. H., Daryono, D., & Wiyono, S. H. (2019). Hypocenter relocation of the aftershocks of the Mw 7.5 Palu earthquake (September 28, 2018) and swarm earthquakes of Mamasa, Sulawesi, Indonesia, using the BMKG network data. Geoscience Letters, 6(1): 1-11. https://doi.org/10.1186/s40562-019-0148-9.
- Supendi, P., Nugraha, A. D., Widiyantoro, S., Pesicek, J. D., Thurber, C. H., Abdullah, C. I., Daryono, D., Wiyono, S. H., Shiddiqi, H. A., & Rosalia, S. (2020). Relocated aftershocks and background seismicity in eastern Indonesia shed light on the 2018 Lombok and Palu earthquake sequences. Geophysical Journal International, 221(3): 1845–1855. https://doi.org/10.1093/gji/ggaa118.
- Cirillo, D., Totaro, C., Lavecchia, G., Orecchio, B., de Nardis, R., Presti, D., Ferrarini, F., Bello, S., & Brozzetti, F. (2022). Structural complexities and tectonic barriers controlling recent seismic activity in the Pollino area (Calabria-Lucania, southern Italy)-constraints from stress inversion and 3D fault model building. Solid Earth, 13(1). https://doi.org/10.5194/se-13-205-2022.
- Zhang, Y., Fadugba, O. I., Powell, C. A., Horton, S. P., & Langston, C. A. (2022). A new madrid seismic zone fault system model from relative event locations and application of optimal anisotropic dynamic clustering. Journal of Geophysical Research: Solid Earth, 127(10). https://doi.org/10.1029/2022jb024194.
- Shelly, D. R., Skoumal, R. J., & Hardebeck, J. L. (2022). s/p amplitude ratios derived from single-component seismograms and their potential use in constraining focal mechanisms for microearthquake sequences. The Seismic Record, 2(2), 118-126. https://doi.org/10.1785/0320220002.
- Vallée, M., Charléty, J., Ferreira, A. M. G., Delouis, B., & Vergoz, J. (2010). Scardec: a new technique for the rapid determination of seismic moment magnitude, focal mechanism and source time functions for large earthquakes using body-wave deconvolution. Geophysical Journal International, 184(1), 338-358. https://doi.org/10.1111/j.1365-246x.2010.04836.x.
- Barth, A., Wenzel, F., & Giardini, D. (2007). Frequency sensitive moment tensor inversion for light to moderate magnitude earthquakes in eastern africa. Geophysical Research Letters, 34(15). https://doi.org/10.1029/2007gl030359.
- Cesca, S., Heimann, S., Stammler, K., & Dahm, T. (2010). Automated procedure for point and kinematic source inversion at regional distances. Journal of Geophysical Research: Solid Earth, 115(B6). https://doi.org/10.1029/2009jb006450.
- Zhang, X., Zhang, M., & Tian, X. (2021). Real-time earthquake early warning with deep learning: application to the 2016 m 6.0 central apennines, italy earthquake. Geophysical Research Letters, 48(5). https://doi.org/10.1029/2020gl089394.

- Yao, Q., Wang, D., Fang, L., & Mori, J. (2019). Rapid estimation of magnitudes of large damaging earthquakes in and around japan using dense seismic stations in china. Bulletin of the Seismological Society of America, 109(6), 2545-2555. https://doi.org/10.1785/0120190107.
- Cheng, Y., Allen, R. M., & Taira, T. (2023). A New Focal Mechanism Calculation Algorithm (REFOC) Using Inter-Event Relative Radiation Patterns: Application to the Earthquakes in the Parkfield Area. Journal of Geophysical Research: Solid Earth, 128(3). https://doi.org/10.1029/2022JB025006.
- Serhalawan, Y., & Chen, P.-F. (2024). Seismotectonics of Sulawesi, Indonesia. Tectonophysics, 883, 230366. https://doi.org/https://doi.org/10.1016/j.tecto.2024.230366.
- Pasari, S., Simanjuntak, A. V. H., Neha, & Sharma, Y. (2021). Nowcasting earthquakes in Sulawesi Island, Indonesia. In Geoscience Letters (Vol. 8, Issue 1). https://doi.org/10.1186/s40562-021-00197-5.
- Huang, H. and Wang, Y. (2022). Seismogenic structure beneath the northern longitudinal valley revealed by the 2018–2021 hualien earthquake sequences and 3-d velocity model. Terrestrial, Atmospheric and Oceanic Sciences, 33(1). https://doi.org/10.1007/s44195-022-00017-z.
- Bratt, S. R., and W. Nagy. (1991). The LocSAT Program, Science Applications International Corporation (SAIC), San Diego, California.
- Hanka, W., Saul, J., Weber, B., Becker, J., & Harjadi, P. (2010). Real-time earthquake monitoring for tsunami warning in the Indian Ocean and beyond. Natural Hazards and Earth System Science, 10(12). https://doi.org/10.5194/nhess-10-2611-2010.
- Kennett, B. L. N., & Engdahl, E. R. (1991). Traveltimes for global earthquake location and phase identification. Geo-physical Journal International, 105(2). https://doi.org/10.1111/j.1365-246X.1991.tb06724.x.
- Kennett, B. L. N., Engdahl, E. R., & Buland, R. (1995). Constraints on seismic velocities in the Earth from traveltimes. Geophysical Journal International, 122(1). https://doi.org/10.1111/j.1365-246X.1995.tb03540.x.
- Jackson, I. (1998). Elasticity, composition and temperature of the earth's lower mantle: a reappraisal. Geophysical Journal International, 134(1), 291-311. https://doi.org/10.1046/j.1365-246x.1998.00560.x.
- Cobden, L., Goes, S., Cammarano, F., & Connolly, J. A. D. (2008). Thermochemical interpretation of one-dimensional seismic reference models for the upper mantle: evidence for bias due to heterogeneity. Geophysical Journal International, 175(2), 627-648. https://doi.org/10.1111/j.1365-246x.2008.03903.x.
- Godwin, H., Waszek, L., & Deuss, A. (2018). Measuring the seismic velocity in the top 15 km of earth's inner core. Physics of the Earth and Planetary Interiors, 274, 158-169. https://doi.org/10.1016/j.pepi.2017.11.010.
- Alamri, A., Rodgers, A., & Alkhalifah, T. (2008). Improving the level of seismic hazard parameters in saudi arabia using earthquake location. Arabian Journal of Geosciences, 1(1), 1-15. https://doi.org/10.1007/s12517-008-0001-5.
- Waldhauser, F., & Ellsworth, W. L. (2000). A Double-difference Earthquake location algorithm: Method and application to the Northern Hayward Fault, California. Bulletin of the Seismological Society of America, 90(6): 1353–1368. https://doi.org/10.1785/0120000006.
- Waldhauser, F. (2001). Hypodd-a program to compute double-difference hypocenter locations. Open-File Report. https://doi.org/10.3133/ofr01113.
- Deemer, W. L., & Olkin, I. (1951). The Jacobians of certain matrix transformations use-ful in multivariate analysis. Biometrika, 38(3–4). https://doi.org/10.1093/biomet/38.3-4.345.
- Díaz-García, J. A., & Gutiérrez-Jáimez, R. (2009). Jacobians of certain transformations of singular matrices. Applica-tiones Mathematicae, 36(2). https://doi.org/10.4064/am36-2-10.
- de Lathauwer, L., de Moor, B., & Vandewalle, J. (2000). A multilinear singular value decomposition. SIAM Journal on Matrix Analysis and Applications, 21(4). https://doi.org/10.1137/S0895479896305696.
- Yutaka, F., Hasemi, A., & Yoshimoto, K. (2008). The detailed hypocenter distribution around the active fault. Zisin (Journal of the Seismological Society of Japan. 2nd Ser.), 61(1), 1-10. https://doi.org/10.4294/zisin.61.1\_1.

- Kilaru, S., Kumar, S., & Dixit, M. M. (2019). Faults plane orientation deduced from the high dense network of short duration data with relocation of hypocenters: koyna-warna region, western india. Open Journal of Earthquake Research, 08(03), 191-200. https://doi.org/10.4236/ojer.2019.83011.
- Piegari, E., Camanni, G., Mercurio, M., & Marzocchi, W. (2024). Illuminating the hierarchical segmentation of faults through an Unsupervised Learning Approach applied to clouds of earthquake hypocenters. Earth and Space Science, 11, e2023EA003267. https://doi.org/10.1029/2023EA003267.
- Lemaire, E., Mreyen, A., Dufresne, A., & Havenith, H. (2020). Analysis of the influence of structural geology on the massive seismic slope failure potential supported by numerical modelling. Geosciences, 10(8), 323. https://doi.org/10.3390/geosciences10080323.
- Sukamto R. (1982). Geological map of the Pangkajene and western part of Watampone Quadrangles, Sulawesi, scale 1:250,000. Geological Research and Development Centre, Bandung, Indonesia.
- Berry, R. F., & Grady, A. E. (1987). Mesoscopic structures produced by Plio-Pleistocene wrench faulting in South Sulawesi, Indonesia. Journal of Structural Geology, 9(5–6). https://doi.org/10.1016/0191-8141(87)90141-6.
- Muzani, M., Nabilla, L., Pratiwi, R. V. E., & Tan, F. (2023). South Sulawesi Arm's Evolution in the Past 50 million years and Its Impacts on the Geology and Geomorphology. Geology, Ecology, and Landscapes, 9(1), 67–79. https://doi.org/10.1080/24749508.2023.2165627.
- van Leeuwen, T. M., Susanto, E. S., Maryanto, S., Hadiwisastra, S., Sudijono, Muhardjo, & Prihardjo. (2010). Tectonostratigraphic evolution of Cenozoic marginal basin and continental margin successions in the Bone Mountains, Southwest Sulawesi, Indonesia. Journal of Asian Earth Sciences, 38(6). https://doi.org/10.1016/j.jseaes.2009.11.005.
- Zhafirah, N. A., HAEDAR, N., SENTOSA, S., & Gani, F. (2024). Micromorphology characterization of crystal calcium carbonate and exopolysaccharides quantification carbonatogenic bacterial ltp4-d isolated from historical painting of maros-pangkep karst area, indonesia. Biodiversitas Journal of Biological Diversity, 25(5). https://doi.org/10.13057/biodiv/d250532.
- Agliardi, F., Dobbs, M. R., Zanchetta, S., & Vinciguerra, S. (2017). Folded fabric tunes rock deformation and failure mode in the upper crust. Scientific Reports, 7(1). https://doi.org/10.1038/s41598-017-15523-1.
- Lloyd, G. E., Halliday, J. M., Butler, R. W. H., Casey, M., Kendall, J. M., Wookey, J., & Mainprice, D. (2011). From crystal to crustal: Petrofabric-derived seismic modelling of regional tectonics. Geological Society Special Publication, 360(1). https://doi.org/10.1144/SP360.4.
- Yamato, P., Duretz, T., & Angiboust, S. (2019). Brittle/ductile deformation of eclogites: insights from numerical models. Geochemistry, Geophysics, Geosystems, 20(7), 3116-3133. https://doi.org/10.1029/2019gc008249.
- Li, Q. and Xu, G. (2012). Tidal triggering of earthquakes in longmen shan region: the relation to the fold belt and basin structures. Earth, Planets and Space, 64(9), 771-776. https://doi.org/10.5047/eps.2011.06.037.
- Yan, X., Zhang, B., Wang, G., Yang, T., & Chen, J. (2023). Coseismic frictional heating with concomitant hydrothermal fluid circulation revealed by rock magnetic properties of fault rocks from the rupture of the 2008 wenchuan earthquake, china. Geochemistry, Geophysics, Geosystems, 24(11). https://doi.org/10.1029/2023gc011223.
- Nonomura, A., Hasegawa, S., Abe, T., Mukoyama, S., & Kaneda, Y. (2021). Validation of an index for susceptibility to earthquake-induced landslides derived from helicopter-borne electromagnetic resistivity and digital elevation data. Geosciences, 11(2), 95. https://doi.org/10.3390/geosciences11020095.
- Maeda, S., Matsuzawa, T., Toda, S., Yoshida, K., & Katao, H. (2018). Complex microseismic activity and depth-dependent stress field changes in wakayama, southwestern japan. Earth, Planets and Space, 70(1). https://doi.org/10.1186/s40623-018-0788-6.
- Li, B. Q. and Du, J. (2020). A methodology for unstructured damped stress inversion of microseismic focal mechanisms: application to the vaca muerta formation, argentina. Geophysics, 85(2), KS39-KS50. https://doi.org/10.1190/geo2019-0275.1.

- 63. Lee, S., Wong, T., Lin, T., & Liu, T. (2019). Complex triggering supershear rupture of the 2018 mw 7.5 palu, indonesia, earthquake determined from teleseismic source inversion. Seismological Research Letters, 90(6), 2111-2120. https://doi.org/10.1785/0220190111.
- 64. Makhnenko, R. and Podladchikov, Y. (2018). Experimental poroviscoelasticity of common sedimentary rocks. Journal of Geophysical Research: Solid Earth, 123(9), 7586-7603. https://doi.org/10.1029/2018jb015685.
- 65. Besharatinezhad, A., Khodabandeh, M. A., Rozgonyi-Boissinot, N., & Török, Á. (2022). The effect of water saturation on the ultrasonic pulse velocities of different stones. Periodica Polytechnica Civil Engineering. https://doi.org/10.3311/ppci.18701.
- 66. Baud, P., Schubnel, A., Heap, M. J., & Rolland, A. (2017). Inelastic compaction in high-porosity limestone monitored using acoustic emissions. Journal of Geophysical Research: Solid Earth, 122(12), 9989. https://doi.org/10.1002/2017jb014627.
- 67. Wells, D. L., & Coppersmith, K. J. (1994). New empirical relationships among magnitude, rupture length, rupture width, rupture area, and surface displacement. Bulletin Seismological Society of America, 84(4). https://doi.org/10.1785/bssa0840040974.
- 68. Leonard, M. (2010). Earthquake fault scaling: Self-consistent relating of rupture length, width, average displacement, and moment release. Bulletin of the Seismological Society of America, 100(5 A). https://doi.org/10.1785/0120090189.
- 69. Stirling, M., Goded, T., Berryman, K., & Litchfield, N. (2013). Selection of earthquake scaling relationships for seismic-hazard analysis. Bulletin of the Seismological Society of America, 103(6). https://doi.org/10.1785/0120130052.
- 70. Purba, J., Restele, L.O., Hadini, L.O., Usman, I., Hasria, H. & Harisma, H. (2024). Spatial study of seismic hazard using classical probabilistic seismic hazard analysis (PSHA) method in the Kendari city area. Indonesian Physical Review, 7 (3): 300–318. https://doi.org/10.29303/ipr.v7i3.325.